Optical Materials 72 (2017) 289–294

Contents lists available at ScienceDirect

Optical Materials

journal homepage: www.elsevier.com/locate/optmat

Distance-dependent metal enhanced fluorescence by flowerlike silver nanostructures fabricated in liquid crystalline phase

Ying Zhang [a, b], Chengliang Yang [a, *], Guiyang Zhang [a, b], Zenghui Peng [a], Lishuang Yao [a], Qidong Wang [a], Zhaoliang Cao [a], Quanquan Mu [a], Li Xuan [a]

[a] State Key Laboratory of Applied Optics, Changchun Institute of Optics, Fine Mechanics and Physics, Chinese Academy of Sciences, Changchun, Jilin, 130033, China

[b] University of Chinese Academy of Sciences, Beijing, 100049, China

ARTICLE INFO

Article history:
Received 14 May 2017
Received in revised form
8 June 2017
Accepted 11 June 2017
Available online 17 June 2017

Keywords:
Metal enhanced fluorescence
Flowerlike silver nanostructure
Localized surface plasmon resonance
Distance-dependent

ABSTRACT

Flowerlike silver nanostructure substrates were fabricated in liquid crystalline phase and the distance dependent property of metal enhanced fluorescence for such substrate was studied for the first time. The distance between silver nanostructures and fluorophore was controlled by the well-established layer-by-layer (LbL) technique constructing alternate layers of poly (allylamine hydrochloride) (PAH) and poly (sodium 4-styrenesulfonate) (PSS). The Rhodamine 6G (R6G) molecules were electrostatically attached to the outmost negative charged PSS layer. The fluorescence enhancement factor of flowerlike nanostructure substrate increased firstly and then decreased with the distance increasing. The best enhanced fluorescence intensity of 71 fold was obtained at a distance of 5.2 nm from the surface of flowerlike silver nanostructure. The distance for best enhancement effect is an instructive parameter for the applications of such substrates and could be used in the practical MEF applications with the flowerlike nanostructure substrates fabricated in such way which is simple, controllable and cost-effective.

1. Introduction

Metal enhanced fluorescence (MEF) is an approach for enhancing the fluorescence intensity of probe molecules nearby the metallic surfaces [1–3]. It is a complex phenomenon combined the effects of enhancement in the emission intensity and quenching of the probe molecules emission. The enhancement is due to the enhanced excitation and radiative decay rate which is induced by the metal nanostructures [1,3]. The quenching of the probe molecules emissions is due to the fact that nonradiative energy transfers to the metal. The probe molecules nearby metallic nanostructures experience enhancement and quenching depend on distance between metallic nanostructures and probe molecules. The distance dependent metal enhanced fluorescence has been theoretically and experimentally studied [4,5]. Lakowicz et al. bound the fluorophores on the 7 nm thick cell membranes, resulting fluorescence signals were enhanced significantly by silver islands films (SIF), while the fluorophores intercalated in the cell nuclei were not influenced significantly by SIF [6,7]. Ginger et al. controlled the distance between silver nanostructures and fluorophores by changing the bond length of complementary deoxyribonucleic acid sequences, and the fluorescence emission intensity was enhanced 13 fold rather than 7 fold with the silver nanostructures without complementary deoxyribonucleic acid sequences [8]. Lakowicz et al. employed multilayer polyelectrolyte of PSS and PAH nanostructures to control the distance. When the distance was 9 nm, the fluorescence intensity was enhanced for 6 fold. However, when the distance was 30 nm, the enhancement was decreased to 1.5 fold [9]. And also, some publications show that the optimal distance should be as large as 60 nm [10]. From above studies we can see that the appropriate distance at which the fluorescence enhancement is the best varies depending on the morphology, shape and size of metallic nanostructures. More and more researchers devoted to flowerlike nanostructure substrates' study owing to its highly effective surface enhanced effects. So far, there are many studies about the best effective distances of silver nanoparticles and silver islands, but there are still little studies about such kind flowerlike silver nanostructure substrate which is a good candidate in the field of MEF. The study of appropriate distance for flowerlike silver nanostructures is still needed especially for applications such as

* Corresponding author.
E-mail address: ycldahai@ciomp.ac.cn (C. Yang).

http://dx.doi.org/10.1016/j.optmat.2017.06.020
0925-3467/

optical imaging, biotechnology and material detections [11–14].

In this work, highly effective surface-enhanced fluorescence substrates with roughened 3D flowerlike silver nanostructures were fabricated by electrodeposition in liquid crystalline template which is stable, simple, controllable, reproductive and cost-effective. Comparing with the silver colloid nanostructures, flowerlike silver nanostructures on substrates are more stable because the silver colloid nanostructures are easy to aggregate under light or heating conditions which vastly influences its applications in optics and material detection. The existing fabrication processes of flowerlike nanostructure substrates in former work are either complicated with expensive machines or instable, while our method needs only one step and very simple machines. We studied the distance-dependent property of MEF from R6G assembled on our flowerlike silver nanostructured substrates using the polyelectrolyte LbL assembly to control the distance from R6G to nanostructures for the first time. In the LbL assembling process, PAH (polycations) and PSS (polyanions) from dilute aqueous solution were sequentially adsorbed onto our silver flowerlike nanostructure substrates by electrostatic interaction. We choose R6G as the fluorophore to investigate the MEF effect which is a kind of very common fluorescence dye in the research field of metal enhanced fluorescence and also be used as laser dye. In order to ensure that the quality of the assembled layers is good, absorption spectra of the assembled layers were measured. And the emission spectra of R6G were also measured. The study shows that fluorescence enhancement factor of flowerlike nanostructure substrate compared with glass substrate experienced an increasing firstly and then decreasing as the distance increases. The best enhancement effect was obtained at the distance of 5.2 nm, which is an instructive parameter for the future applications of such substrates and should be considered in all MEF applications similar in this work.

2. Theory

Fluorescence is a character for a material to absorb light at a wavelength and emit light of longer wavelength, which is due to the radiative relaxation from an electronically excited state [1]. The process includes two parts which are absorption and emission of light. The two aspects were quantified by excitation efficiency and fluorescence quantum yield, respectively. According to the Jablonski diagram, the final fluorescence emission intensity is determined by the product of these two factors mentioned above. Excitation efficiency is influenced by the intensity of excitation light and fluorescence quantum yield (Q_o) is determined by the radiative (Γ) and nonradiative decay rates (k_{nr}) [1] which can be described by

$$Q_o = \frac{\Gamma}{\Gamma + k_{nr}}. \tag{1}$$

Metal enhanced fluorescence is an approach for enhancing the fluorescence intensity of fluorophores nearby the metallic surfaces which is due to the localized surface plasmon resonance from the collective oscillation of electrons. The fluorescence enhancement can then be described by

$$\frac{\gamma_{em}}{\gamma^o_{em}} = \frac{\gamma_{exc}}{\gamma^o_{exc}} \frac{Q}{Q_o} \tag{2}$$

where γ_{em} and γ^o_{em} are the fluorescence rates of a single molecule with and without metal nanostructures, respectively. γ_{exc} and γ^o_{exc} are the excitation rates with and without metal nanostructures, respectively. γ_{exc} is proportional to $|\mathbf{E}\cdot\mathbf{p}|$, in which $\mathbf{E}$ is the local electric field and $\mathbf{p}$ is the transition dipole moment. Q and Q_o are the quantum yields with and without metal nanostructures, respectively. Q can be expressed as

$$Q = \frac{\Gamma + \Gamma_m}{\Gamma + \Gamma_m + k_m + k_{nr}} \tag{3}$$

where Γ_m and k_m are additional radiative and nonradiatvie decay rates of the excited molecule in the presence of metal nanostructures. In summary, the enhancement effect could be attributed to three competing effects: (1) local field enhancement on the surface of metal nanostructures enhanced the excitation rate leading to enhanced excitation efficiency. (2) surface plasmon-coupled emission from coupling of the fluorescence emission with the metal nanostructures causes increase of radiative decay rate (Γ_m), which leads to the increased quantum yield. (3) the non-radiative energy transfer from the fluorophores to metal nanostructures leading to increased non-radiative decay rate (k_m) which results in fluorescence quenching [1,2,15,16]. These three effects fall off when the distance between fluorophore and metal nanostructure increases. According to studies before, the non-radiative energy transfer effect dominates at the surface and drops off with inverse third power of distance, while the local field effect decays exponentially from the surface [15]. Therefore, an appropriate distance can be found at which the enhancement of local field and the quenching effect could achieve a balance to realize the best fluorescence enhancement effect.

3. Experimental methods

3.1. Materials

Anionic surfactant sodium bis (2-ethylhexyl) sulfosuccinate (AOT) (98wt %), oil phase p-xylene (99wt %), silver nitrate (99wt %) and PSS were from Sigma-Aldrich. PAH and Silver foil (2.0 mm 99%) were obtained from Alfa Aesar. Cysteamine (95wt %) was obtained from Macklin. R6G was purchased from J&K (China). Deionized water was obtained from the Millipore Elixir 100 and the resistivity is over 18MΩ·cm. All of the materials were used as received.

3.2. Preparation of flowerlike silver nanostructure substrates

In the past decades, lyotropic liquid crystal have been investigated because of its remarkable effects on structure and morphology of desired nanomaterials [17,18]. Flowerlike silver nanostructures grown on the ITO glass by means of electrodeposition in liquid crystalline phase was reported previously by us [19]. The liquid crystalline phase was prepared according to the ternary phase diagram [20] consisting of AOT, oil phase of p-xylene and water which was replaced by $AgNO_3$ aqueous solution for the growth of silver flowers. In the electrodeposition process, a silver foil was mounted as the anode with an indium tin oxide (ITO) glass ($15 \times 40\ mm^2$) whose surface was very smooth was mounted as the cathode to collect the flowerlike silver structure. And the liquid crystalline phase was used as the electrolyte. The applied 3.0 V potential was controlled by a DC voltage-stabilized power supply. After the deposition, the negative electrode ITO glass was softly washed by ethanol and dried by a gentle flow of N_2.

3.3. Adsorption of polyelectrolyte layers and R6G

Negatively charged PSS and positively charged PAH were used as the spacers between nanostructures and R6G. It was realized through layer by layer assembling owing to electrostatic interaction between oppositely charged polyelectrolytes. Cysteamine was used to functionalize the silver nanostructure substrates with amines and positively charge the substrates before PSS/PAH multilayer

adsorption. A cation dye R6G could be electrostatically attached to the negatively charged PSS layer. The molecular structures are shown in Fig. 1.

The flowerlike silver nanostructure substrates were immerged in 1 mM cysteamine in ethanolic solution for 24 h and then washed with plenty of ethanol and deionized water. By this step, the surfaces of silver nanostructure substrates were functionalized with a self-assembled monolayer of cysteamine. These positively charged substrates were used for polyelectrolyte PSS deposition which was a polyanion. Then the substrates were immersed in a PSS solution with concentration of 3 mg/mL for 20 min followed by a wash in deionized water for 5 min. After this step, there was a self-assembled monolayer of PSS on the surface of cysteamine layer. Then the substrates were immersed again in the PAH solution with concentration of 2 mg/mL for 20 min, followed by a wash in deionized water for 5 min. After which, the monolayer of PAH was self -assembled on the surface of the PSS layer. The thickness of each layer of PSS/PAH was about 2.1 nm [9]. Multilayer assemblies were obtained by adsorption of PSS/PAH layers. The different distances between silver nanostructures and R6G molecules could be controlled by depositing different number layers of PSS/PAH. A schematic process of multilayer film formation is shown in Fig. 2. The outmost layer of PSS was used for immobilization of R6G by electrostatic interaction. Half (only a PSS layer) to four and a half layers of PSS/PAH with distances of approximately 1, 3.1, 5.2, 7.3 and 9.4 nm respectively were obtained by adsorption of both polyelectrolytes. After the layers were dried, R6G molecules were adsorbed onto the PSS layer by immersion into an aqueous R6G solution for 2 h followed by drying at ambient condition. Meanwhile, R6G molecules were adsorbed onto the glass substrate by immersion into an aqueous R6G solution for 2 h and then the immersed glass substrate was used as the reference substrate.

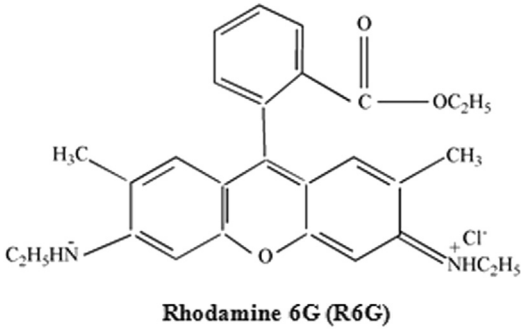

Fig. 1. Molecular structures of Rhodamine 6G, PSS, Cysteamine, PAH.

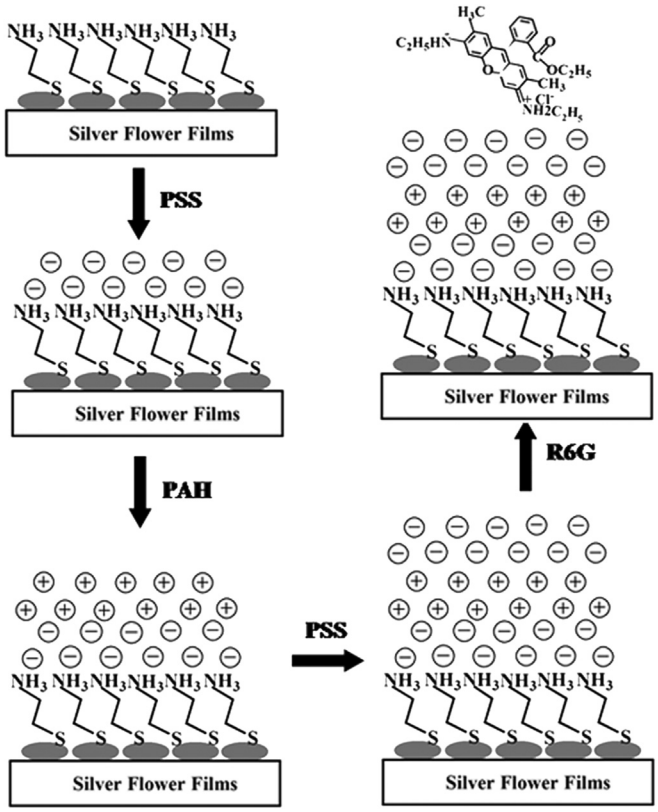

Fig. 2. The process of layer by layer assembly of polyelectrolytes and R6G.

3.4. Spectroscopic measurement

In this work, the absorption spectra were used to characterize the PSS/PAH layer. Because the absorptions are the same for PSS/PAH layers of the same thickness, absorption spectra were used to determine the amounts of PSS and PAH bound to silver nanostructure substrates which can show the quality of the LbL assembled films and improve the reliability of distance [5].

According to the study of Krishanu Ray's group [21], the photophysical characteristics of some dyes adsorbed on different substrates could be different which is determined by the concentration of the dyes and adsorption process. In order to ensure the optical characteristics of R6G molecules adsorbed on silver substrates, LbL assembled silver substrates and glass substrate were not changed, adsorption spectra and emission spectra were employed.

Absorption spectra were from the UV-3101PC UV-VIS-NIR scanning spectrophotometer. Emission spectra of the R6G assembled on different substrates were recorded by a Hitachi F4500 fluorescence spectrophotometer using 514 nm excitation wavelength.

4. Results and discussion

4.1. Morphology of flowerlike silver nanostructure

The morphology of the silver nanostructure was observed with field emission scanning electron microscope (FESEM) S-4800 from HITACHI. The FESEM pictures of the flowerlike silver nanostructures are shown in Fig. 3. The fabricated silver structure is quite like a rose with a highly roughened surface composed of high density petals whose thickness is about 50 nm. Between the petals there are many horns and thin gaps which are favorable for 'hot spots'. The size of the flower is about 2 μm.

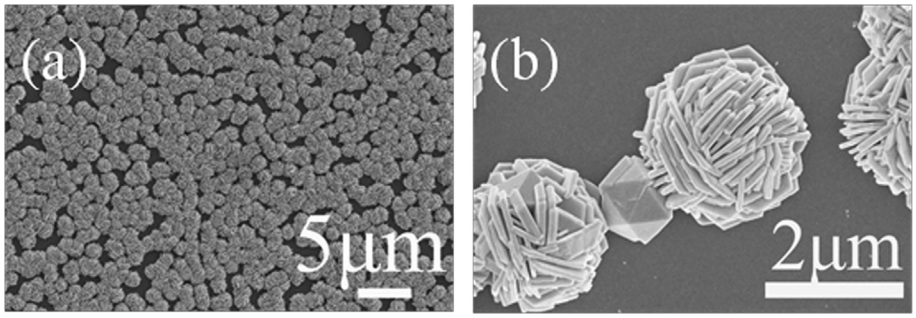

Fig. 3. FESEM pictures of the flowerlike silver nanostructures. (a) is the photo of nanostructures with low magnification. (b) is the magnified picture.

4.2. Spectral results

4.2.1. Absorbance of PSS/PAH layers

To study the distance dependence MEF of R6G on flowerlike silver nanostructure substrates, we employed the layer by layer technique to control the distance between silver nanostructures and R6G molecules. Constructions of PSS/PAH layers on silver nanostructure substrate were achieved as described in the Experimental Method section. The quality and thickness of PSS/PAH layers were checked by the absorption spectra as Fig. 4 shows. Fig. 4(a) shows the absorption spectra of flowerlike silver nanostructure substrates with different layers of LbL films. Fig. 4(b) shows the increased absorption of silver substrates with LbL films at 514 nm compared with silver substrate without LbL films. As we can see, the absorptions of the substrates with 0.5, 1.5, 2.5, 3.5, 4.5 layers of PSS/PAH increase linearly with the layer number increasing. But compared with the zero layer substrate, the absorption of substrate with 0.5 layer of PSS/PAH intensely increase.

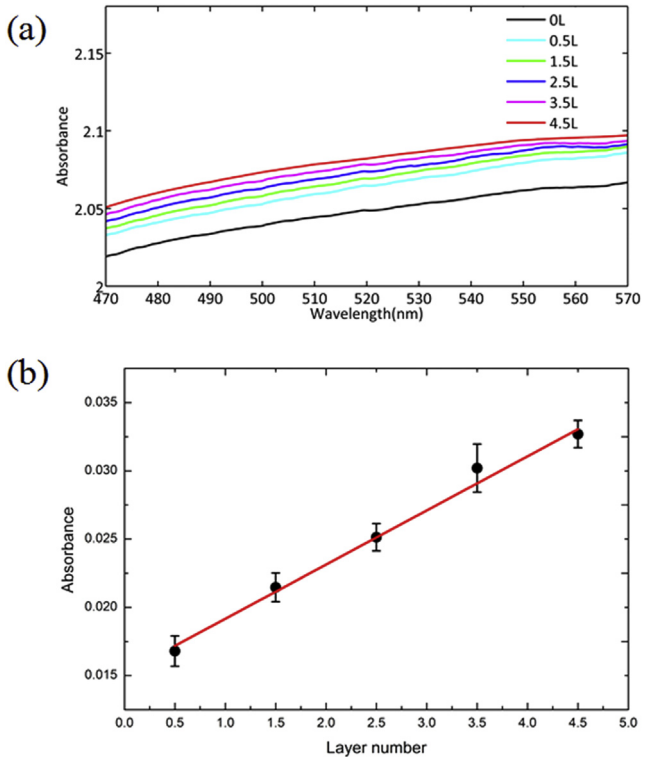

Fig. 4. Absorbance spectra of flowerlike silver nanostructure substrates with different layers of PSS/PAH. (a) absorption spectra. (b) increased absorption of silver substrates with LbL films at 514 nm compared with silver substrate without LbL films.

We think this effect can be attributed to the cysteamine layer which was adsorbed on the silver substrate before LbL assembling. In other words, the absorption increase of the substrate with 0.5 layer of PSS/PAH was not only from PSS layer, but also cysteamine layer. The absorption increases linearly with the number of PSS/PAH layers and absorption of each layer is also consistent with monolayer, which indicates that the quality of assembled layers are good and the thickness of each layer is almost the same. In order to ensure the thickness of the PSS/PAH bilayer was the same as Ref. [9], we calculated the thickness of one PSS/PAH bilayer by comparing our measured optical density of each PSS/PAH bilayer with the published data in the former work [22]. The optical density of 0.005 was added for each PSS/PAH bilayer whose thickness was about 3.8 ± 0.3 nm in the Ref. [22]. In our experiment, the optical density of about 0.003 was added for each PSS/PAH bilayer. According to the Beer-Lamber Law, optical density is directly proportional to the thickness of the film. The calculated thickness of PSS/PAH bilayer in our experiment was about 2.28 ± 0.18 nm which scope includes 2.1 nm we used in the paper.

4.2.2. Photophysical properties of R6G on different substrates

In order to guarantee the photophysical property of R6G molecules absorbed on glass substrate, silver nanostructure substrate and LbL assembled silver nanostructure substrate are the same, we measured their absorption and emission spectra.

The absorption properties of R6G on different substrates are shown in Fig. 5. Fig. 5 (a) (b) and (c) show the absorption spectra of different substrates before and after adsorbing R6G molecules. The black lines show the absorption characters of different substrates before adsorbing R6G molecules and the red ones represent the absorption characters after adsorbing R6G molecules. Fig. 5(a), (b) and (c) show the absorption characters of glass substrate, Ag substrate and LbL assembled silver substrate before and after adsorbing R6G molecules, respectively. From the results, we can see that after adsorbing R6G, the absorptions of different substrates all increase due to the R6G molecules' absorption. In order to study the absorption characters of R6G adsorbed on different substrates, we employed the relative absorption spectra of R6G subtracting the spectra of non-adsorbed substrates for different substrates. Fig. 5(d) shows the absorption spectra of R6G molecules adsorbed on different substrates. From the results, we observe that the peaks of adsorption spectra are the same on 543 nm, and the shapes of them are similar while the absorbance spectra intensities are a little different which we think results from the silver film and self -assembled layers. The process for forming the self-assembled PSS/PAH bilayer ensures the quality of the outmost layer of PSS is good. The properties of PSS layers on different substrates are the same. The methods and conditions for R6G adsorption for different substrates are the same. So the densities of R6G molecules should be same on different substrates. Considering, we choose the excitation

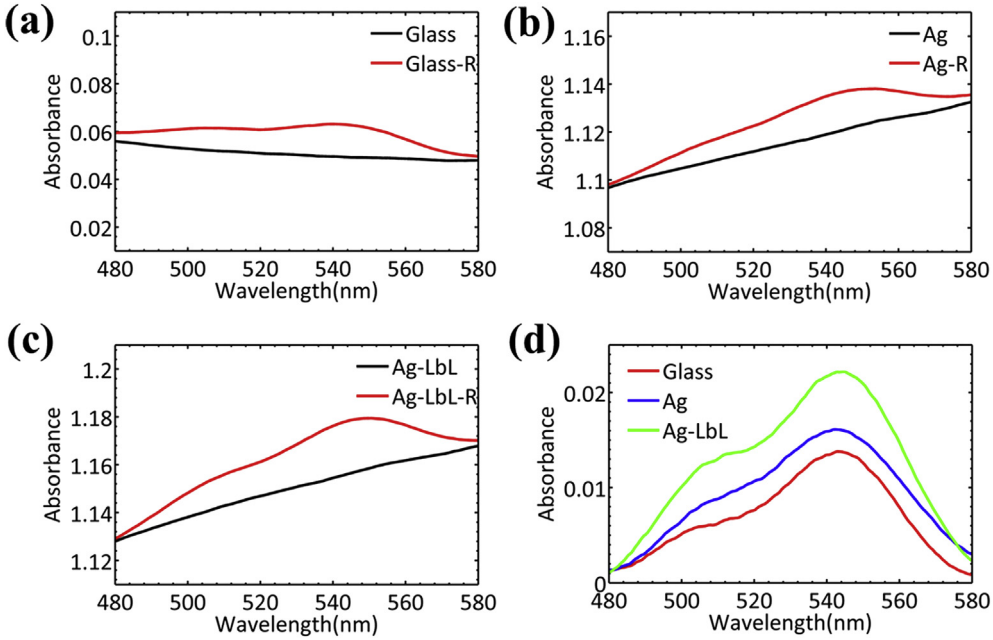

Fig. 5. Absorption spectra of different substrates. (a) is absorption spectra of glass substrate before and after adsorbing R6G. (b) is absorption spectra of Ag substrate before and after adsorbing R6G. (c) is absorption spectra of LbL assembled silver substrate before and after adsorbing R6G. (d) is the absorption spectra of R6G subtracting the spectra of non-adsorbed substrates for different substrates.

light with 514 nm at which the absorbance character of R6G molecules adsorbed on different substrates are the same. Normalized emission spectra of R6G on LbL film assembled silver substrate, silver substrate and glass substrate are shown in Fig. 6. They all have an emission peak at 561 nm and the spectra are almost the same. According to the very similar R6G absorption spectra and emission spectra on different substrates, we think the photophysical properties of R6G are the same on different substrates.

4.2.3. Metal enhanced fluorescence effect

The enhancement effects of such silver nanostructure substrates have already been studied in our former work which shows that the reproducibility is good [23]. The absorption spectra of LbL films indicate that the quality of assembled layers is good and the method of controlling distances is reliable. The consistency of absorption property and emission property of R6G layers adsorbed on different substrates ensure that the photophysical characters of R6G on different substrates are the same. The effects mentioned above which may have influences on the final enhancement result are excluded before the metal enhanced fluorescence experiments.

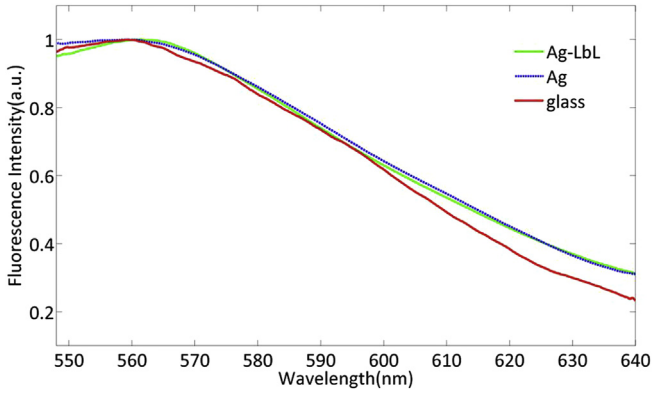

Fig. 6. Normalized emission spectra of R6G on glass substrate, silver substrate, LbL assembled silver substrate, respectively.

We performed a series of experiments on R6G absorbed PSS/PAH layers assembled on flowerlike silver nanostructure substrates where the distance between R6G and surface of nanostructure varied from 0 to 9.4 nm. Fluorescence emission spectra from R6G adsorbed PSS/PAH layers at different distances are shown in Fig. 7 (a). Fluorescence intensities of R6G show significant changes. The enhancement factors are calculated as follows

$$E_f = \frac{I_{Ag-substrate} - I_{Ag-background}}{I_{reference} - I_{reference-background}} \quad (4)$$

where $I_{Ag\text{-}substrate}$ is the fluorescence intensity of R6G on the substrates with flowerlike silver nanostructures and $I_{reference}$ is the fluorescence intensity on the glass substrate. $I_{Ag\text{-}background}$ and $I_{reference\text{-}background}$ are noise signals generated by sliver substrate and glass substrate, respectively.

The enhancement factors are plotted as a function of the metal–fluorophore distance and they are shown in Fig. 7(b). We can see that the enhancement factor increases from 46 fold to 71 fold with the distance increasing from 0 to 5.2 nm and reduces from 71 to 50 with the distance increasing from 5.2 to 9.4 nm. The best enhanced effect is obtained with 2.5 layers of PSS/PAH which indicates that the distance from the silver nanostructure surface to the R6G is 5.2 nm.

The results show that metal enhanced fluorescence of flowerlike silver nanostructures is distance dependent. According to the theory introduced in the Theory section, the decrease of fluorescence intensity below and above 5.2 nm could be attributed to the quenching of emission when the R6G molecules are close to the silver surface and the drops of local field enhancement effect respectively. Firstly, local field enhancement on the surface of metal nanostructures enhanced the excitation efficiency which leads to fluorescence enhancement. From the SEM photo, the silver nanostructure is quite like a rose composed of high density petals and between which there are many horns and thin gaps, which are favorable for 'hotspots'. The enhanced local field close to the silver surface enhanced the excitation energy which motivates the excitation efficiency of R6G increase. Secondly, the excited R6G

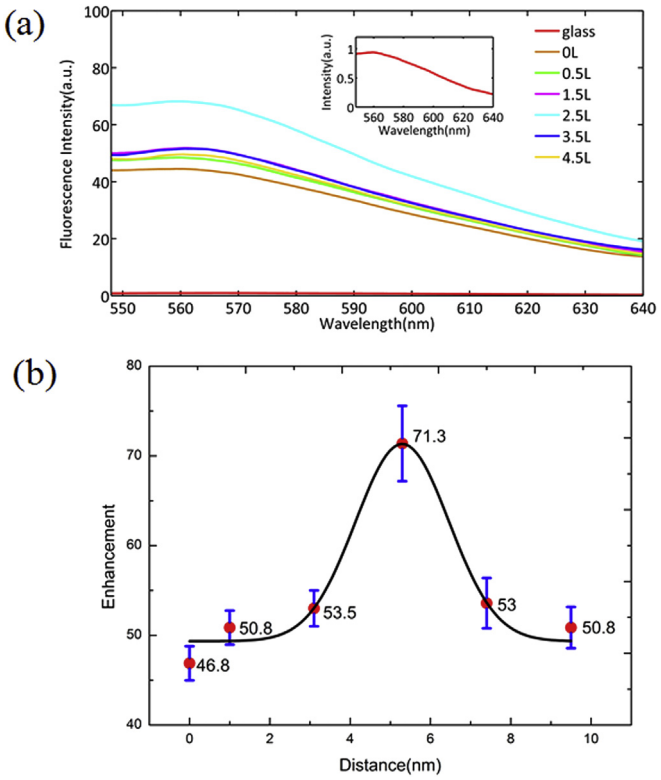

Fig. 7. The metal enhanced fluorescence intensity of different distances from the metal nanostructure surface to the R6G. (a) is the fluorescence spectra of R6G. (b) is the enhancement factors with different distances.

molecules which were not de-excitation by radiating fluorescence transfer their energy to nearby silver flower excitating surface plasmon. The surface plasmon radiates the same wavelength radiation as the fluorescence radiated by the fluorophore molecules with a larger radiative efficiency compared with the fluorophore. The effect increases the radiative decay rate and quantum yield of the fluorophore which leads to fluorescence enhancement. Thirdly, the non-radiative energy transfer from the fluorophores to metal nanostructures leading to increased non-radiative decay rate resulting in fluorescence quenching. When the distance is large enough, the induced charges distribution on the interface is sparse, which leads to radiating. When the distance is small, the induced charges distribution on the interface is dense, which leads to energy loss rather than radiating. The quenching depends on the distance between the silver surface and R6G with an inverse third power of distance. The enhanced local field and decreased quenching reaches a best balance resulting in a best fluorescence enhancement effect in the distance of 5.2 nm in this experiment.

5. Conclusion

In this work, we fabricated the highly effective metal enhanced fluorescence substrate of flowerlike silver nanostructures in liquid crystalline phase and studied its distance dependent property of metal enhanced fluorescence using LbL technique for the first time. We controlled the distance between metal surface and fluorophore from 0 to 9.4 nm by a polyelectrolyte alternate LbL assembly technique. The reliability of distance controlling and the consistency of photophysical characters of R6G absorbed on different substrates were verified by absorption and emission spectra. The enhancement factor increased firstly and then decreased with the distance increasing which indicates that the enhanced effect is distance dependent. The maximum fluorescence enhancement factor of 71 fold was achieved at a distance of 5.2 nm. The enhanced fluorescence caused by localized surface plasmon resonance and fluorescence quenching reaches a best balance. The results from this work could be used in the practical MEF application with such flowerlike silver nanostructure substrate especially in optical imaging, biotechnology and material detection fields.

Acknowledgements

This work is supported by the National Natural Science Foundation of China, with grant numbers 11204299, 61205021, Foundation of State Key Laboratory of Applied Optics, Changchun Institute of Optics, Fine Mechanics and Physics, and Youth Innovation Promotion Association Chinese Academy of Sciences.

References

[1] E. Fort, S. Grésillon, Surface enhanced fluorescence, J. Phys. D Appl. Phys. 41 (2008) 013001.
[2] J.R. Lakowicz, Radiative decay engineering 5: metal-enhanced fluorescence and plasmon emission, Anal. Biochem. 337 (2005) 171–194.
[3] J.R. Lakowicz, K. Ray, M. Chowdhury, H. Szmacinski, Y. Fu, J. Zhang, K. Nowaczyk, Plasmon-controlled fluorescence: a new paradigm in fluorescence spectroscopy, Analyst 133 (2008) 1308–1346.
[4] P. Anger, P. Bharadwaj, L. Novotny, Enhancement and quenching of single-molecule fluorescence, Phys. Rev. Lett. 96 (2006) 113002.
[5] J. Malicka, I. Gryczynski, Z. Gryczynski, J.R. Lakowicz, Effects of fluorophore-to-silver distance on the emission of cyanine–dye-labeled oligonucleotides, Anal. Biochem. 315 (2003) 57–66.
[6] K. Ray, M.H. Chowdhury, J.R. Lakowicz, Observation of surface plasmon-coupled emission using thin platinum films, Chem. Phys. Lett. 465 (2008) 92–95.
[7] J. Zhang, Y. Fu, D. Liang, R.Y. Zhao, J.R. Lakowicz, Enhanced fluorescence images for labeled cells on silver island films, Langmuir 24 (2008) 12452–12457.
[8] Y. Chen, K. Munechika, D.S. Ginger, Dependence of fluorescence intensity on the spectral overlap between fluorophores and plasmon resonant single silver nanoparticles, Nano Lett. 7 (2007) 690–696.
[9] K. Ray, R. Badugu, J.R. Lakowicz, Polyelectrolyte layer-by-layer assembly to control the distance between fluorophores and plasmonic nanostructures, Chem. Mater. 19 (2007) 5902–5909.
[10] K. Sokolov, G. Chumanov, T.M. Cotton, Enhancement of molecular fluorescence near the surface of colloidal metal films, Anal. Chem. 70 (1998) 3898–3905.
[11] Q. Sun, K. Ueno, H. Yu, A. Kubo, Y. Matsuo, H. Misawa, Direct imaging of the near field and dynamics of surface plasmon resonance on gold nanostructures using photoemission electron microscopy, Light-Sci. Appl. 2 (2013) e118.
[12] J. Malicka, I. Gryczynski, J.R. Lakowicz, DNA hybridization assays using metal-enhanced fluorescence, Biochem. Bioph. Res. Co. 306 (2003) 213–218.
[13] N. Li, A. Tittl, S. Yue, H. Giessen, C. Song, B. Ding, N. Liu, DNA-assembled bimetallic plasmonic nanosensors, Light-Sci. Appl. 3 (2014) e226.
[14] H. Jung, M. Park, M. Kang, K.-H. Jeong, Silver nanoislands on cellulose fibers for chromatographic separation and ultrasensitive detection of small molecules, Light-Sci. Appl. 5 (2016) e16009.
[15] W. Ge, X. Zhang, M. Liu, Z. Lei, R. Knize, Y. Lu, Distance dependence of gold-enhanced upconversion luminescence in Au/SiO 2/Y 2 O 3: Yb 3+, Er 3+ nanoparticles, Theranostics 3 (2013) 282–288.
[16] H. Sharma, M.A. Digman, N. Felsinger, E. Gratton, M. Khine, Enhanced emission of fluorophores on shrink-induced wrinkled composite structures, Opt. Mater. Express 4 (2014) 753–763.
[17] C. Wang, D. Chen, X. Jiao, Lyotropic liquid crystal directed synthesis of nanostructured materials, Sci. Technol. Adv. Mater. 10 (2009) 023001.
[18] B. Yin, J. Liu, X. Wei, D. Sun, Color liquid crystals formed in cationic surfactant/n-butanol/water system, Chin. J. Liq. Cryst. Disp. 3 (2005) 003.
[19] C. Yang, X. Xiang, Y. Zhang, Z. Peng, Z. Cao, J. Wang, L. Xuan, Large-scale controlled fabrication of highly roughened flower-like silver nanostructures in liquid crystalline phase, Sci. Rep-UK 5 (2015) 12355.
[20] P. Ekwall, L. Mandell, K. Fontell, Solubilization in micelles and mesophases and the transition from normal to reversed structures, Mol. Cryst. Liq. Cryst. 8 (1969) 157–213.
[21] K. Ray, H. Nakahara, Adsorption of sulforhodamine dyes in cationic Langmuir-Blodgett films: spectroscopic and structural studies, J. Phys. Chem. C 106 (2002) 92–100.
[22] J.J. Harris, M.L. Bruening, Electrochemical and in situ ellipsometric investigation of the permeability and stability of layered polyelectrolyte films, Langmuir 16 (2000) 2006–2013.
[23] Y. Zhang, C. Yang, X. Xiang, P. Zhang, Z. Peng, Z. Cao, Q. Mu, L. Xuan, Highly effective surface-enhanced fluorescence substrates with roughened 3D flowerlike silver nanostructures fabricated in liquid crystalline phase, Appl. Surf. Sci. 401 (2017) 297–305.